Robust 2-Qubit Gates in a Linear Ion Crystal Using a Frequency-Modulated Driving Force

Pak Hong Leung,[1,*] Kevin A. Landsman,[2] Caroline Figgatt,[2] Norbert M. Linke,[2]
Christopher Monroe,[2,4] and Kenneth R. Brown[1,3]
[1]School of Physics, Georgia Institute of Technology, Atlanta, Georgia 30332, USA
[2]Joint Quantum Institute and Joint Center for Quantum Information and Computer Science, University of Maryland, College Park, Maryland 20742, USA
[3]Schools of Chemistry and Biochemistry and Computational Science and Engineering, Georgia Institute of Technology, Atlanta, Georgia 30332, USA
[4]IonQ Inc., College Park, Maryland 20742, USA

(Received 30 August 2017; revised manuscript received 30 October 2017; published 9 January 2018)

In an ion trap quantum computer, collective motional modes are used to entangle two or more qubits in order to execute multiqubit logical gates. Any residual entanglement between the internal and motional states of the ions results in loss of fidelity, especially when there are many spectator ions in the crystal. We propose using a frequency-modulated driving force to minimize such errors. In simulation, we obtained an optimized frequency-modulated 2-qubit gate that can suppress errors to less than 0.01% and is robust against frequency drifts over ±1 kHz. Experimentally, we have obtained a 2-qubit gate fidelity of 98.3(4)%, a state-of-the-art result for 2-qubit gates with five ions.

DOI: 10.1103/PhysRevLett.120.020501

Ion traps are a leading candidate for the realization of a quantum computer. Magnetically insensitive qubit energy splittings, long coherence times, and high-fidelity state initialization and detection [1,2] prove to be significant advantages for trapped ion qubits. Individual qubit addressing and single-qubit gates with error rates on the order of 10^{-5} per gate have been achieved [1,3–5]. Multiple qubits can be entangled through state-dependent forces driven by external fields [6–9], and for exactly two ions, entangling gate fidelities routinely exceed 99% and in some cases 99.9% [10–15].

With increasing ion number, however, the motional modes bunch in frequency, which means exciting only a single motional mode becomes prohibitively slow. Alternatively, the state-dependent driving forces can couple to all modes of motion. A number of schemes have been proposed for disentangling the internal qubit states from the motional states of all modes by introducing variations to the driving force during the gate. One way to achieve this goal is amplitude modulation (AM) of the driving field [16,17]. Several experiments have adopted this method and have achieved a 2%–5% error [18–20]. Discrete phase modulation (PM) has also been proposed for the same purpose, but the number of pulses in the sequence increases exponentially with the number of ions [21]. Moreover, discrete changes in laser amplitude and phase are hard to implement physically, especially when we perform fast gates.

We propose a novel decoupling method through continuous frequency modulation (FM), theoretically equivalent to continuous PM, which involves only small and smooth oscillations of the detuning of the applied field. First, we explain the coherent displacement of the ion chain's motional modes during the Mølmer-Sørensen (MS) gate. Then, we describe how the residual displacement of the ions can be minimized in a way which is robust to small changes in trap frequency. Next, we experimentally demonstrate this gate in a chain of five $^{171}Yb^{+}$ ions. Finally, we discuss extensions of the method to larger ion chains, with 17 ions as an example.

To entangle two qubits with the MS gate, we apply a state-dependent driving force near the sideband frequencies. As a result, each motional mode experiences a coherent displacement characterized by the operator [16,17]:

$$\hat{D}(\hat{\alpha}_k) = \exp(\hat{\alpha}_k a_k^\dagger - \hat{\alpha}_k^\dagger a_k),$$
$$\hat{\alpha}_k(t) = \frac{\Omega}{2}(\eta_{i,k}\sigma_\phi^i + \eta_{j,k}\sigma_\phi^j)\int_0^t e^{i\theta_k(t')}dt', \quad (1)$$

where Ω is the carrier coupling strength, $\eta_{i,k}$ and $\eta_{j,k}$ are the Lamb-Dicke parameters of ions i and j with respect to mode k, σ_ϕ^i and σ_ϕ^j are bit-flip Pauli operators for the addressed ions, and $\theta_k(t) = \int_0^t \delta_k(t')dt'$ and $\delta_k(t)$ are the phase and detuning of the driving force relative to mode k. If the qubits are at the $+1$ eigenstate of both σ_ϕ^i and σ_ϕ^j, the displacement is

$$\alpha_k(t) = \frac{\Omega}{2}(\eta_{i,k} + \eta_{j,k})\int_0^t e^{i\theta_k(t')}dt'. \quad (2)$$

We may visualize the trajectory of $\alpha_k(t)$ over time by plotting it in the complex plane. This is the phase space

trajectory (PST) of the motional mode k. For a total gate time τ, $\alpha_k(0) = 0$ and $\alpha_k(\tau)$ are the beginning and end points of the PST.

Because of the state-dependent nature of $\hat{\alpha}_k(t)$, different eigenstates of σ_ϕ^i and σ_ϕ^j follow different PSTs. If any of the $\alpha_k(\tau)$ is nonzero, there is residual entanglement between the internal and motional state spaces, which leads to a mixed internal state. This lowers the overall gate fidelity ($F = |\langle\psi_{\text{final}}|\psi_{\text{ideal}}\rangle|^2$). Given that $|\alpha_k| \ll 1$, we find that the consequent gate error may be estimated as

$$\varepsilon \equiv 1 - F \approx \sum_{k=1}^{N} |\alpha_k(\tau)|^2. \tag{3}$$

Minimizing $|\alpha_k|$ is therefore the most straightforward criterion for an optimized gate. However, the gate is sensitive to small drifts in sideband frequencies ($\delta_k \to \delta_k + \delta_1$ and $\delta_1 \ll 1/\tau$), an imperfection which we often observe in experiments. The frequency dependence of $\alpha_k(\tau)$ can be canceled to the first order by setting the time-averaged position of $\alpha_k(t)$ to zero:

$$\alpha_{k,\text{av}} \propto \int_0^\tau \int_0^t e^{i\theta_k(t')} dt' dt = 0. \tag{4}$$

It turns out that if we only consider symmetric pulses [$\delta_k(\tau - t) = \delta_k(t)$], minimizing $\alpha_{k,\text{av}}$ also minimizes $\alpha_k(\tau)$.

In our scheme, we modulate the driving frequency during the gate to minimize the gate error. The trajectory $\alpha_k(t)$ moves with constant speed but varying angular rate $\delta_k(t)$. Therefore, FM allows us to control the curvature and thus the shapes and end points of the PSTs. We let the frequency assume a symmetric, oscillatory pattern (see example in Fig. 1). The vertices (local maxima and minima) of the oscillations are set to be evenly spaced in time and are the only variable control parameters in our optimization. The vertices are connected with sinusoidal functions, which leads to a smooth and continuous frequency profile. The function to be minimized is $|\alpha_{k,\text{av}}|^2$ for robust pulses and $|\alpha_k|^2$ for nonrobust pulses. The number of vertices used is increased until we successfully converge to a solution with errors much lower than 0.01%. Detailed derivations for Eqs. (3) and (4) as well as the optimization process are provided in the Supplemental Material [22].

Both robust and nonrobust versions of the gate are tested on our five-ion quantum computer. In our setup, five $^{171}\text{Yb}^+$ ions are held in a rf Paul trap with a radial trap frequency of 3.045 MHz and an average ion separation of about 5 μm. Our qubit is defined by the ground hyperfine states $^2S_{1/2}, |F = 0\rangle$ and $^2S_{1/2}, |F = 1\rangle$ with an energy splitting of $2\pi \times 12.642821$ GHz [1]. Initially, all ions are cooled to close to the motional ground state ($\approx$0.1 phonons) and then optically pumped to the $|0\rangle$ state. Quantum gates are implemented using a beat note generated by counterpropagating Raman laser beams that are capable of addressing any individual qubit [18].

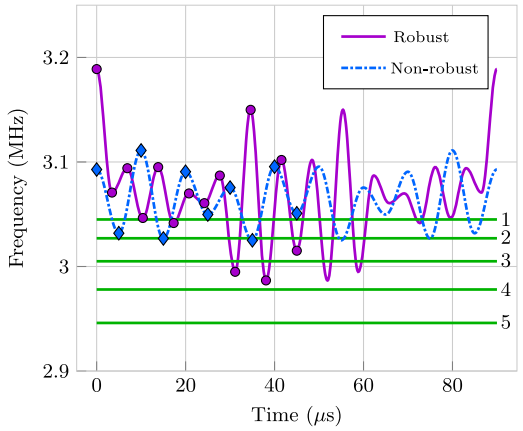

FIG. 1. Robust (violet, solid line) and nonrobust (blue, dash-dotted line) FM pulses for 2-qubit gate optimized for five ions, both with a gate time of 90 μs. Green lines are experimental sideband frequencies, labeled 1–5, the first one being the common mode frequency. The pulses are designed to be symmetric in time. The dots and diamonds are the vertices of the frequency and represent the control parameters allowed to vary in our optimization algorithm.

The five transverse motional sidebands are experimentally determined and used to find the optimal FM pulses for the 2-qubit gate. We increase the number of oscillations (degrees of freedom) for optimization until we find a pulse with low errors. With a fixed gate time of 90 μs, the optimized robust pulse consists of 13 oscillations, whereas the nonrobust version has only nine (Fig. 1). The driving frequency crosses the sidebands multiple times, which contrasts with other implementations of MS gates that avoid sideband resonance.

PSTs are plotted for no frequency error and for a 1 kHz frequency drift for both robust and nonrobust pulses in Fig. 2. With the drift, the end points of the robust trajectory (circles) stick to the origin, whereas those of the nonrobust (diamonds) deviate from the starting point, causing an estimated error of about 0.5%. This proves the importance of the robustness criterion.

We present the results on entangling two neighboring ions on one edge of the ion chain in the robust case. The output population and parity are measured and shown in Figs. 3(a) and 3(b), giving a fidelity of 98.3(4)%, excluding state preparation and measurement (SPAM) errors. This is among the highest fidelities achieved for multiqubit gates in the presence of spectator ions [18]. Using the robust gate, we also successfully perform a CNOT gate with 98.6(7)% fidelity and generate a 3-qubit GHZ state with 92.6(3)% fidelity. The 1% error level observed is partially attributed to laser intensity fluctuations (~2%), which breaks the assumption of constant laser power during the gate.

In order to lower the overall laser intensity Ω, each 90 μs pulse is performed twice for each gate, with a combined gate time of 180 μs. The Ω required is $2\pi \times 600$ kHz in carrier Rabi frequency, which is much larger than

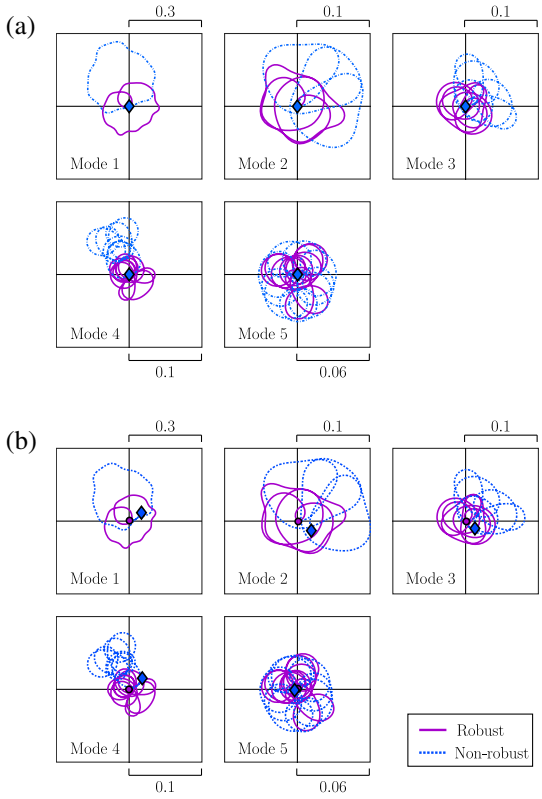

FIG. 2. Simulated PSTs with (a) no frequency error and (b) −1 kHz sideband drift, using the FM pulses shown in Fig. 1. The end points for the robust pulse (circles) return to the starting point with the drift, whereas those for the nonrobust pulse (diamonds) fail to do so. The horizontal and vertical axes represent the quadratures $x_k \sim a_k^\dagger + a_k$ and $p_k \sim i(a_k^\dagger - a_k)$, respectively.

$2\pi \times 151$ kHz as expected by simulation. The discrepancy is most likely due to an overestimate of the Lamb-Dicke parameters in our simulation. The high power used worsens other error sources such as Raman scattering, off-resonant excitation, and cross talk with other qubits [11,12].

The theoretically estimated gate error is plotted as a function of frequency drift in Fig. 4(a) to compare the robust pulse with the nonrobust pulse. A typical error threshold for high-fidelity gates is 0.01%. The robust pulse can tolerate frequency errors up to ±1.5 kHz, whereas the nonrobust less than ±0.1 kHz. The nonrobust pulse has a quadratic dependence on the drift, whereas the robust version has a quartic dependence. This is expected, since error is proportional to displacement squared, and the first-order dependence of the displacement on drift is canceled out in the robust case.

To determine the impact of sideband drifts, we experimentally run the two gates over a range of symmetric detuning offsets [Fig. 4(b)]. The robust version has even-parity population higher than 90% for frequency offsets up to ±5 kHz, whereas the nonrobust gate has significantly lower fidelity and tolerance towards frequency errors (within ±1 kHz), confirming that the robust method improves

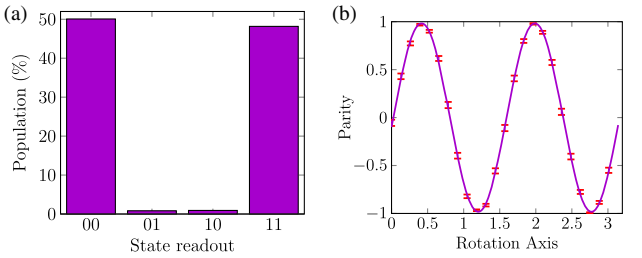

FIG. 3. (a) State population and (b) parity scan of the two qubits after the optimized and robust 2-qubit gate shown in Fig. 1, indicating a fidelity of 98.3(4)%.

fidelity significantly by canceling errors due to frequency drifts.

To test the scalability of our method, we run a similar optimization for 17 ions, motivated by the 17-qubit surface code proposed for quantum error correction [23–26]. The sideband frequencies are calculated from a simulated anharmonic ion trap with an average ion separation of about 3.5 μm. Such high ion density may be challenging to realize with current technology, but that does not pose a fundamental physical limit to experiments.

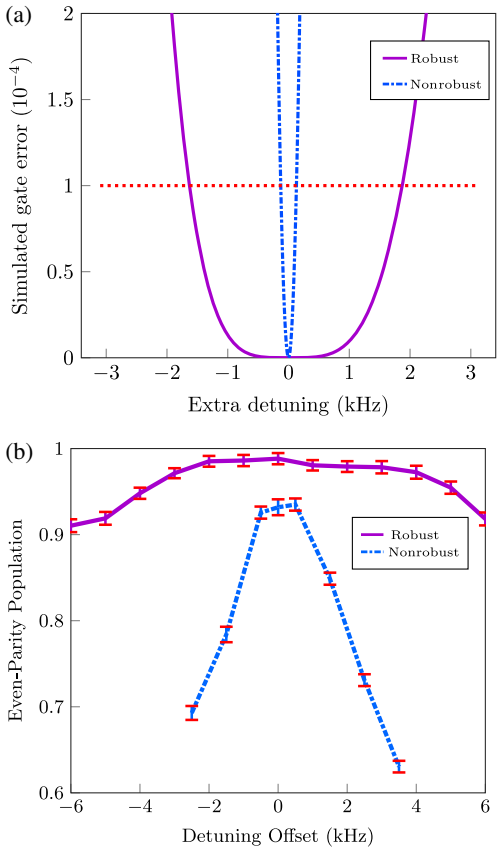

FIG. 4. (a) Simulated gate error and (b) experimental even-parity populations of the two qubits after the gate for a range of detuning offsets. The robust gate has a significantly better performance than the nonrobust gate in both theory and experiment.

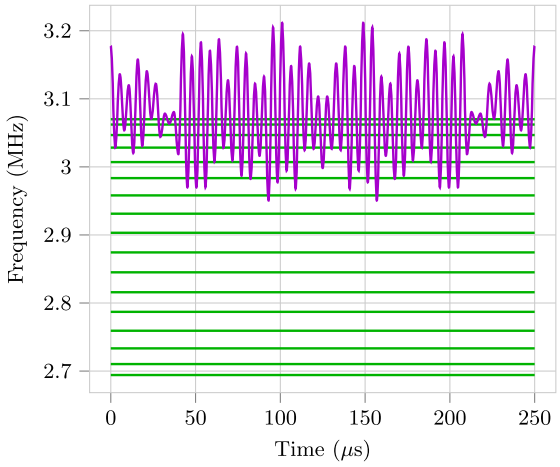

FIG. 5. Optimized FM 2-qubit gate for 17 ions. The sideband frequencies (green) are obtained by simulations.

The robust FM pulse obtained consists of 47 oscillations within a gate time of 250 μs (Fig. 5). The gate can tolerate a frequency drift of 500 Hz for an error threshold of 0.01%. Apparently, the gate is more sensitive to frequency errors due to an increased number of motional modes and a longer gate time.

The power required (Ω) for the 2-qubit gate ranges from $2\pi \times 115$ kHz for neighboring ions to $2\pi \times 249$ kHz for the furthest separated ions ($\approx 1:2$ ratio between lowest and highest). This is an encouraging result. Previous simulation results indicate that 2-qubit gate time and power increase very quickly with the distance between the ions. But by using a flexible and well-designed optimization program, we have found a FM pulse that can overcome this difficulty.

We have shown that we can perform high-fidelity 2-qubit gates in a five-ion trap using frequency modulation. In theory, the optimized robust FM pulse can suppress errors in gate fidelities to below 0.01% for up to a ± 1.5 kHz frequency offset for five $^{171}Yb^{+}$ ions. The gate is used to maximally entangle two ions in experiment and has a fidelity of 98.3(4)%. We speculate that in the near future, we will attain over 99.9% fidelity previously achieved with two-ion chains [10–12].

We would like to thank Todd Green, Luming Duan, and Gang Shu for useful discussions. This work was supported by the Office of the Director of National Intelligence–Intelligence Advanced Research Projects Activity through ARO Contract No. W911NF-10-1-0231 and the ARO MURI on Modular Quantum Systems.

*pleung6@gatech.edu

[1] S. Olmschenk, K. C. Younge, D. L. Moehring, D. N. Matsukevich, P. Maunz, and C. Monroe, Phys. Rev. A **76**, 052314 (2007).
[2] R. Noek, G. Vrijsen, D. Gaultney, E. Mount, T. Kim, P. Maunz, and J. Kim, Opt. Lett. **38**, 4735 (2013).
[3] K. R. Brown, A. C. Wilson, Y. Colombe, C. Ospelkaus, A. M. Meier, E. Knill, D. Leibfried, and D. J. Wineland, Phys. Rev. A **84**, 030303 (2011).
[4] T. P. Harty, D. T. C. Allcock, C. J. Ballance, L. Guidoni, H. A. Janacek, N. M. Linke, D. N. Stacey, and D. M. Lucas, Phys. Rev. Lett. **113**, 220501 (2014).
[5] D. P. L. Aude Craik, N. M. Linke, M. A. Sepiol, T. P. Harty, J. F. Goodwin, C. J. Ballance, D. N. Stacey, A. M. Steane, D. M. Lucas, and D. T. C. Allcock, Phys. Rev. A **95**, 022337 (2017).
[6] K. Mølmer and A. Sørensen, Phys. Rev. Lett. **82**, 1835 (1999).
[7] A. Sørensen and K. Mølmer, Phys. Rev. Lett. **82**, 1971 (1999).
[8] G. Milburn, S. Schneider, and D. F. V. James, Fortschr. Phys. **48**, 801 (2000).
[9] E. Solano, R. L. de Matos Filho, and N. Zagury, Phys. Rev. A **59**, R2539 (1999).
[10] V. M. Schäfer, C. J. Ballance, K. Thirumalai, L. J. Stephenson, T. G. Ballance, A. M. Steane, and D. M. Lucas, arXiv:1709.06952.
[11] C. J. Ballance, T. P. Harty, N. M. Linke, M. A. Sepiol, and D. M. Lucas, Phys. Rev. Lett. **117**, 060504 (2016).
[12] J. P. Gaebler, T. R. Tan, Y. Lin, Y. Wan, R. Bowler, A. C. Keith, S. Glancy, K. Coakley, E. Knill, D. Leibfried, and D. J. Wineland, Phys. Rev. Lett. **117**, 060505 (2016).
[13] C. Ospelkaus, U. Warring, Y. Colombe, K. R. Brown, J. M. Amini, D. Leibfried, and D. J. Wineland, Nature (London) **476**, 181 (2011).
[14] T. P. Harty, M. A. Sepiol, D. T. C. Allcock, C. J. Ballance, J. E. Tarlton, and D. M. Lucas, Phys. Rev. Lett. **117**, 140501 (2016).
[15] T. Monz, P. Schindler, J. T. Barreiro, M. Chwalla, D. Nigg, W. A. Coish, M. Harlander, W. Hänsel, M. Hennrich, and R. Blatt, Phys. Rev. Lett. **106**, 130506 (2011).
[16] S.-L. Zhu, C. Monroe, and L.-M. Duan, Europhys. Lett. **73**, 485 (2006).
[17] C. F. Roos, New J. Phys. **10**, 013002 (2008).
[18] S. Debnath, N. M. Linke, C. Figgatt, K. A. Landsman, K. Wright, and C. Monroe, Nature (London) **536**, 63 (2016).
[19] K. Kim, M.-S. Chang, R. Islam, S. Korenblit, L.-M. Duan, and C. Monroe, Phys. Rev. Lett. **103**, 120502 (2009).
[20] T. Choi, S. Debnath, T. A. Manning, C. Figgatt, Z.-X. Gong, L.-M. Duan, and C. Monroe, Phys. Rev. Lett. **112**, 190502 (2014).
[21] T. J. Green and M. J. Biercuk, Phys. Rev. Lett. **114**, 120502 (2015).
[22] See Supplemental Material at http://link.aps.org/supplemental/10.1103/PhysRevLett.120.020501 for more detailed derivations and experimental results.
[23] C. J. Trout, M. Li, M. Gutierrez, Y. Wu, S.-T. Wang, L. Duan, and K. R. Brown, arXiv:1710.01378.
[24] Y. Tomita and K. M. Svore, Phys. Rev. A **90**, 062320 (2014).
[25] C. Horsman, A. G. Fowler, S. Devitt, and R. V. Meter, New J. Phys. **14**, 123011 (2012).
[26] A. M. Stephens, Phys. Rev. A **89**, 022321 (2014).